

Triply-Differential Photoelectron Studies of Molecular Autoionization Profiles: The 710–730 Å Region of the N₂ Spectrum

A. C. Parr, D. L. Ederer, and B. E. Cole^(a)

Synchrotron Ultraviolet Radiation Facility, National Bureau of Standards, Washington, D. C. 20234

and

J. B. West

Daresbury Laboratory, Science Research Council, Daresbury, Warrington WA4 4AD, England

and

Roger Stockbauer

Surface Science Division, National Bureau of Standards, Washington, D. C. 20234

and

Keith Codling

J. J. Thomson Physical Laboratory, University of Reading, Reading RG6 2AF, England

and

J. L. Dehmer

Argonne National Laboratory, Argonne, Illinois 60439

(Received 25 August 1980)

Photoelectron studies of molecular autoionization resolved into position within the resonance profile, photoelectron ejection angle, and final vibrational state are reported. By using the first members of prominent window and absorption series converging to N₂⁺ B²Σ_u⁺ as an example, striking variations of vibrational branching ratios and photoelectron asymmetry parameters within autoionizing profiles are demonstrated. Such triply differential data represent a very detailed characterization of the rovibronic interactions governing molecular autoionization.

PACS numbers: 33.80.Eh, 33.60.-q

Autoionization is a window onto aspects of photoelectron dynamics which are often too subtle to be readily seen in direct photoionization. Resolving the autoionization into photoelectron ejection angle further enhances its sensitivity by bringing into play the phases of coupling strengths as well.¹ The only previous systematic measurements of angularly resolved autoionization were made by Samson and Gardner² on the *ns* and *nd* Rydberg series between the ²P_{1/2, 3/2} fine-structure thresholds of atomic xenon. Agreement with predictions¹ was good, but there were discrepancies. These have very recently been largely accounted for by a more sophisticated calculation³ of the key dynamical parameters. One of the main lessons learned from this early work on atoms is that angularly resolved autoionization profiles can provide a much more stringent test of our theoretical understanding than profiles in the total cross section.

Molecular autoionization spectra have the additional richness of the vibrational and rotational degrees of freedom: Now electronic excitation

can be exchanged not only among different electronic channels, but with molecular vibration and rotation as well.⁴ The molecular case is correspondingly richer and the theory is more complicated. The first calculation was made on the pure rotational autoionization spectrum in H₂.⁵ Recently the analysis has been extended to treat simultaneous vibrational and rotational autoionization in H₂, leading to the prediction of pronounced changes of the spectral profiles with rotational/vibrational decay channel,⁶ and with angle.⁷ These workers expect the same general features to emerge in the full treatment of simultaneous rotational-vibrational-electronic (rovibronic) autoionization.⁸ While no branching ratio or angularly resolved data for H₂ are yet available for direct comparison, the good agreement between these calculations and the high-resolution photoionization data of Dehmer and Chupka⁹ suggest the general validity of these predictions.

In this context, the experiments which we report here and theory approach one another. Molecular hydrogen is accessible to the theorists be-

cause the key dynamical parameters are available from analysis of discrete spectra.¹⁰⁻¹³ There is in H_2 , however, no appreciable electronic autoionization. In N_2 , on the other hand, electronic autoionization is dominant, vibrational decay modes provide a substructure, and rotational effects are not resolved at all. It is our view that N_2 represents the prototype molecular system wherein the full rotational-vibrational-electronic autoionization process is in play and that its analysis will form the basis of the detailed, general treatment of molecular autoionization.

The main purpose of this Letter, therefore, is to illustrate the striking variations of partial cross sections and photoelectron asymmetry parameters both as a function of position within a resonance and as a function of final vibrational channel. We hope this example will stimulate direct theoretical analysis, since comprehensive mapping of triply differential studies of autoionization in nitrogen and other simple molecules now appears entirely feasible and likely with the successful utilization of synchrotron radiation.

The apparatus used in this work has been described in detail elsewhere¹⁴ and will only be briefly discussed here. The variable-wavelength light was obtained from a large-aperture 2-m, normal-incidence monochromator¹⁵ attached to the National Bureau of Standards (SURF-II) storage ring. With a 1200-line/mm grating, a virtual entrance slit (the stored electron orbit) and a 200- μ m exit slit, this instrument produced a spectral resolution of 0.8 Å full width at half maximum (FWHM) and a flux of 10^{11} photons/sec at 600 Å with 10 mA circulating in the storage ring. The ejected electrons were energy analyzed by a 2-in.-mean-radius hemispherical analyzer¹⁶ operated at a constant resolution of 100 meV. The analyzer was calibrated with use of Ar gas whose photoionization cross section and photoelectron asymmetry parameters are known in this wavelength range. As the light from the monochromator was elliptically polarized, the differential cross section in the dipole approximation, by assuming randomly oriented target molecules, can be written^{14,17}

$$d\sigma_i/d\Omega = (\sigma_{\text{tot}}/4\pi)[1 + \frac{1}{4}\beta(3P \cos 2\theta + 1)], \quad (1)$$

where β is the photoelectron asymmetry parameter, θ is the photoelectron ejection angle relative to the major polarization axis, and $P = (I_{\parallel} - I_{\perp}) / (I_{\parallel} + I_{\perp})$ is the polarization of the light which was measured with a three-mirror polarization analyzer.¹⁴ At each wavelength reported here, elec-

tron spectra encompassing and completely resolving the vibrational progression of the $N_2^+ \ ^2\Sigma_g^+$ final ionic state were recorded at $\theta = 0^\circ$, 45° , and 90° . Angular distributions and (magic angle) vibrational branching ratios were determined directly from these measurements by using Eq. (1).

This prototype study focuses on the first members of the prominent absorption and "emission" or window series converging to the $v=0$ level of $N_2^+ \ B^2\Sigma_u^+$ at 661.2 Å. Three series have been observed in this region (see, e.g., Refs. 18-22): The strong Hopfield absorption series¹⁸ with a quantum defect of ~ 0.07 ,¹⁹ together with a strong series of window resonances, the Hopfield "emission" series, with a weak absorption series shadowing it on the long-wavelength side. The quantum defects of these latter two series are in the range $\sim 0.85-0.95$.¹⁹ Several assignments have been made in this spectral range (see, e.g., Refs. 19, 23-27) and, although none are unequivocally established, we follow Ogawa and Tanaka¹⁹ in assigning the Rydberg electron in the Hopfield absorption series to $nd\sigma_g$ and that in the other weak-absorption series to $ns\sigma_g$. This is consistent with quantum defects and oscillator strengths in a recent model calculation,²⁷ which showed that an $nd\pi_g$ series is also very close to the $ns\sigma_g$ and together they would account for the weak absorption and window series. Clearly these spectroscopic questions will have to be definitively answered as a first step in analyzing the triply differential data presented here. In the present work, we focus on the first members of these series which lie in the wavelength range 710-730 Å and focus mainly on the principal absorption peak (723.3 Å) and window resonance (715.5 Å) without attempting to specifically correlate features in our data with the weak absorption series or other faint structure in this range.

In Fig. 1, we present the vibrational branching ratios for formation of the ground-state ion $N_2^+ \ X^2\Sigma_g^+$ by photoionization in the range $710 \text{ \AA} \leq \lambda \leq 730 \text{ \AA}$. Here we define the vibrational branching ratio as the ratio of the intensity of a particular vibrational level to the sum over the whole vibrational band. In Fig. 2 the asymmetry parameter β is given for the same processes. In both figures the positions of the Hopfield emission and absorption features at 715.5 and 723.3 Å, respectively, are indicated by solid lines joining the upper and lower frames. In the vicinity of these features, a hand-drawn dashed curve is constructed only to guide the eye, and should not be taken too seriously. In both figures, typical error

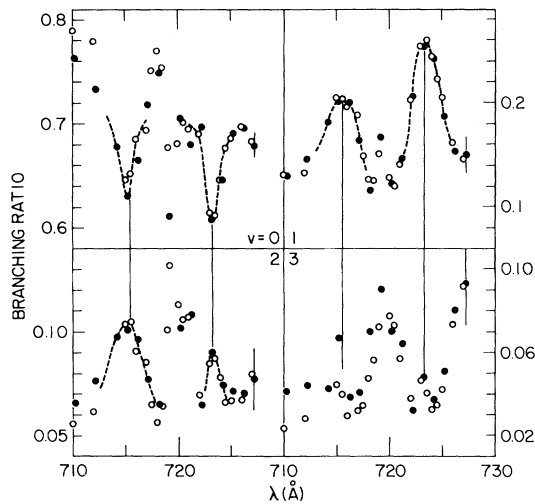


FIG. 1. Vibrational branching ratios for production of $N_2^+ X^2 \Sigma_g^+$ ($v = 0-3$) in the range $710 \text{ \AA} \leq \lambda \leq 730 \text{ \AA}$. Vertical lines at 715.5 and 723.3 \AA denote the positions of the first members of the Hopfield "emission" and absorption series (Ref. 18) approaching the $N_2^+ B^2 \Sigma_u^+$ ($v = 0$) limit. Typical error bars are indicated on the last point in each frame. The dashed line is hand drawn to guide the reader's eye. Open and closed circles represent two independent runs (see text).

bars for the data in each frame are shown on the last point. Duplicate branching ratio measurements (the open circles were taken at the magic angle and the solid dots were deduced from the angular distribution measurements) show the reproducibility of the data. Note that an early branching-ratio study of this vicinity of the N_2 photoionization spectrum was reported by Woodruff and Marr,²⁸ but without angle dependence and with insufficient wavelength resolution and sensitivity to characterize the profiles of the Hopfield resonances.

Focusing first on the vibrational branching ratios in Fig. 1, we see three major qualitative features:

(1) The $v=0$ branching ratio exhibits pronounced dips at the location of the two major autoionization features, whereas the higher vibrational channels, most notably $v=1$, show enhancements. Hence, the quasibound autoionizing states mediate a transfer of dipole amplitude from the $v=0$ channel, dominant in direct photoionization, to the much weaker $v=1, 2$, and 3 channels. This transfer is primarily directed to the $v=1$ channel and is much diminished by $v=3$. This enhancement of vibrational channels with small Franck-Condon factors relative to the most in-

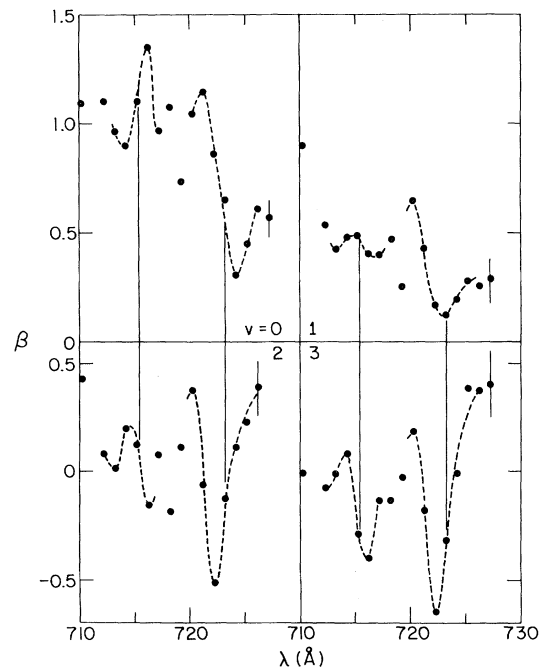


FIG. 2. Photoelectron asymmetry parameters corresponding to producing $N_2^+ X^2 \Sigma_g^+$ ($v = 0-3$) in the range $710 \text{ \AA} \leq \lambda \leq 730 \text{ \AA}$. Other conventions as for Fig. 1.

tense channel is consistent with the effect of a shape resonance in those few cases studied so far (see, e.g., Refs. 29-31). From another point of view, the observation may simply reflect a $\Delta v = \pm 1$ propensity rule, such as observed⁶ for vibrational autoionization in H_2 , where the $\Delta v = -1$ transitions dominate, irrespective of the Franck-Condon factors for direct photoionization. Establishing the systematics of this diverse set of observations is obviously a most timely problem.

(2) Despite the great contrast between the window and absorption profiles in the photoabsorption and photoionization spectra, the profiles in Fig. 1 are of similar shape and both exhibit either an enhancement or depletion, depending upon the channel.

(3) Definite "interloper" structure occurs between the two major resonances, with variable shape and strength. Both the weak absorption peak near the window resonance and other weak structures (one peak in the photoionization spectrum²² at 718.8 \AA correlates well with the main interloper structures in Fig. 1) may play a role here.

The angular distribution results in Fig. 2 also exhibit structure at the positions of the two major resonances and in between. Implicit in the spec-

tral variations in β is information on both the vibrational branching ratios and the relative phases of the alternative vibrational ionization channels. Specifically, the competition between asymptotic phases produces large asymmetric variations in β at the resonance positions, which vary from one final vibrational level to another. For instance, the β curve near the Hopfield "emission" line exhibits a peak for $v=0$ which evolves into a dip for $v=3$. Near the Hopfield absorption profile, the position of the minimum in β , although not extremely well defined by these data, clearly shifts from the long-wavelength side of the resonance position to the short-wavelength side.

We conclude by reiterating that triply differential data of this type will soon be produced in increasing volume, due largely to the advent of high-resolution, angle-resolving, electron spectrometers utilizing synchrotron light sources. Our group has already followed this prototype measurement with studies of O_2 and CO , and more extensive work on N_2 . It would therefore be most timely to develop the theoretical tools, analogous to those in Refs. 6-8, for application to the full rovibronic description of molecular autoionization, in order to extract the wealth of detailed dynamical information contained in this type of data.

We are indebted to Dan Dill for helping us place this work in the context of recent theoretical developments. We would also like to thank R. P. Madden for his support and encouragement, and the staff of the National Bureau of Standards SURF-II facility for their valuable assistance. This work was supported in part by U. S. Office of Naval Research and by the U. S. Department of Energy.

^(a)Present address: Honeywell Corporate Technology Center, Bloomington, Minn. 55420.

¹D. Dill, Phys. Rev. A 7, 1976 (1973).

²J. A. R. Samson and J. L. Gardner, Phys. Rev. Lett. 31, 1327 (1973).

³W. R. Johnson, K. T. Cheng, K.-N. Huang, and M. LeDourneuf, Phys. Rev. A 22, 989 (1980).

⁴D. Dill and Ch. Jungen, J. Phys. Chem. 84, 2116 (1980); Ch. Jungen and D. Dill, J. Chem. Phys. 73,

3338 (1980).

⁵D. Dill, Phys. Rev. A 6, 160 (1972).

⁶M. Raoult and Ch. Jungen, J. Chem. Phys. (to be published).

⁷M. Raoult, Ch. Jungen, and D. Dill, J. Phys. Chim. (to be published).

⁸D. Dill and Ch. Jungen, to be published.

⁹P. M. Dehmer and W. A. Chupka, J. Chem. Phys. 65, 2243 (1976).

¹⁰U. Fano, Phys. Rev. A 2, 353 (1970).

¹¹G. Herzberg and Ch. Jungen, J. Mol. Spectrosc. 41, 425 (1972).

¹²O. Atabek, D. Dill, and Ch. Jungen, Phys. Rev. Lett. 33, 123 (1974).

¹³O. Atabek and Ch. Jungen, in *Electron and Photon Interactions with Atoms*, edited by H. Kleinpoppen and M. R. C. McDowell (Plenum, New York, 1975); Ch. Jungen and O. Atabek, J. Chem. Phys. 66, 5584 (1977).

¹⁴A. C. Parr, Roger L. Stockbauer, B. E. Cole, D. L. Ederer, J. L. Dehmer, and J. B. West, Nucl. Instrum. Methods 172, 357 (1980).

¹⁵D. L. Ederer, B. E. Cole, and J. B. West, Nucl. Instrum. Methods 172, 185 (1980).

¹⁶J. L. Dehmer and D. Dill, Phys. Rev. A 18, 164 (1978).

¹⁷J. A. R. Samson and A. F. Starace, J. Phys. B 8, 1806 (1975).

¹⁸J. J. Hopfield, Phys. Rev. 35, 1133 (1930), and 36, 789 (1930).

¹⁹M. Ogawa and Y. Tanaka, Can. J. Phys. 40, 1593 (1962).

²⁰R. E. Huffman, Y. Tanaka, and J. C. Larrabee, J. Chem. Phys. 39, 910 (1963).

²¹P. Gurtler, V. Saile, and E. E. Koch, Chem. Phys. Lett. 48, 245 (1977).

²²P. M. Dehmer and W. A. Chupka, to be published.

²³R. S. Mulliken, Phys. Rev. 46, 144 (1934).

²⁴H. Lefebvre-Brion and C. M. Moser, J. Chem. Phys. 43, 1394 (1965).

²⁵E. Lindholm, Ark. Fys. 40, 111 (1969).

²⁶T. Betts and V. McKoy, J. Chem. Phys. 54, 113 (1971).

²⁷W. Kosman, P. M. Dehmer, J. L. Dehmer, D. Dill, and S. Wallace, to be published.

²⁸P. R. Woodruff and G. V. Marr, Proc. Roy. Soc. London, Ser. A 358, 87 (1977).

²⁹R. Stockbauer, B. E. Cole, D. L. Ederer, J. B. West, A. C. Parr, and J. L. Dehmer, Phys. Rev. Lett. 43, 757 (1979).

³⁰J. L. Dehmer, D. Dill, and S. Wallace, Phys. Rev. Lett. 43, 1005 (1979).

³¹J. B. West, A. C. Parr, B. E. Cole, D. L. Ederer, R. Stockbauer, and J. L. Dehmer, J. Phys. B 13, L105 (1980).